Chrysanthemum Foliar Necrosis: Transmission Electron Microscopy of Leaf Lesions

M. M. Dienelt and R. H. Lawson

Florist and Nursery Crops Laboratory, Beltsville Agricultural Research Center, USDA, Beltsville, MD 20705.
Accepted for publication 2 April 1991 (submitted for electronic processing).

ABSTRACT

Dienelt, M. M., and Lawson, R. H. 1991. Chrysanthemum foliar necrosis: Transmission electron microscopy of leaf lesions. Phytopathology 81:1079-1087.

Plants of the Marble cultivars of *Dendranthema grandiflora* (formerly *Chrysanthemum* × *morifolium*) often display necrotic spotting of lower leaves and premature leaf senescence. Ultrastructural cytopathology from leaves of cultivars Pink Marble, White Marble, and Florida Marble was compared with that of leaf tissue from unaffected chrysanthemum cultivars Vero, Fanfare, Surf, and Bonnie Jean. P-protein and plastid complexes in sieve elements of the Marble cultivars were often highly electron-dense and sieve and companion cell obliteration sometimes appeared enhanced over controls. Mature sieve elements contained endoplasmic reticulum, plasmalemmae, plastids with starch grains, mitochondria, vesicles, and P-protein. Mycoplasmalike organisms were not observed. Necrosis was distinguished by collapse of mesophyll and epidermal cells, formation of papillae-like appositions on cell walls bordering necrosis, and accumulations of electron-dense spherical or filamentoid substances in central vacuoles. Similar features were present in necrotic foliar lesions from Vero, Fanfare, and Bonnie Jean treated with toxic levels of manganese. Results are consistent with earlier evidence indicating that chrysanthemum foliar necrosis in the Marble cultivars is associated with manganese toxicity and not a biotic agent.

Additional keywords: Chrysanthemum phloem necrosis.

The Marble cultivars of the florist's chrysanthemum, *Dendranthema grandiflora* Tzveler (formerly *Chrysanthemum* × *morifolium* Ramat.), often develop necrotic spotting of lower leaves and premature leaf senescence (20,21). Abnormal inflorescences with green bracts in the disk also may occur. The syndrome has been attributed to a mycoplasmalike organism (MLO) that causes the disease chrysanthemum phloem necrosis (CPN) (11,20–22). There is evidence, however, that low levels of manganese can induce similar foliar symptoms (4,16,17). In addition, similar floral symptoms have been widely reported in many chrysanthemum cultivars affected by heat delay, a condition caused by high temperatures during floral initiation (25).

We initiated a series of studies evaluating the Marble cultivars for presence of a graft-transmissible agent (17), sensitivity to manganese (17), and the effect of temperature on floral anatomy (18). This paper describes two areas of investigation: examination of tissues from the Marble cultivars for the presence of an MLO and comparison of the cytopathology of the Marbles with that of confirmed manganese toxicity in other chrysanthemum cultivars.

MATERIALS AND METHODS

Source plants and culture. *D. grandiflora* cvs. Florida Marble, Pink Marble, and White Marble with and without symptoms of foliar necrosis were compared, using symptomless cvs. Bonnie Jean, Fanfare, and Vero as controls. Rooted cuttings were grown in a mixture of mineral soil, perlite, and peat moss (2:1:1). Plants were fertilized with a proportioner injector every 2 wk with 200 ppm Peters 20-20-20 (N-P-K), starting 2 wk after potting, and were treated with 100 ml of an aqueous solution of $MnSO_4$ ranging from 0.6 g/L to 4.8 g/L every 2 wk. Foliar symptoms were compared with untreated controls. Each test was repeated at least twice over a period of 2 yr. In most experiments, plants were grown in a greenhouse with temperatures fluctuating from 18 to 30 C. During winter, plants were exposed to 14 h of supplemental incandescent light to prevent flowering.

Sampling and processing of plants for MLO evaluation. Samples were taken from symptomatic (as well as asymptomatic) leaves of Pink Marble, Florida Marble, and White Marble plants grown without supplemental manganese or lime. Fully expanded mature leaves, partially expanded young leaves, and fully expanded leaves midway between the two were sampled. Plants of unaffected cvs. Vero, Fanfare, Surf, and Bonnie Jean sampled from similar leaf positions served as controls. Experiments were repeated two to five times, with six replicates per experiment.

Processing and fixation followed protocols used previously to preserve MLO structure (13). Leaf pieces no larger than 2 mm square were placed in 4 C in 2% glutaraldehyde and 1.5% acrolein in 0.05 M Na_2HPO_4-KH_2PO_4 buffer, pH 7.0. After postfixing in 1% OsO_4 in the same buffer, samples were dehydrated in ethyl alcohol and propylene oxide and embedded in LX112. Ultrathin sections were stained for 45 min with uranyl acetate and for 15 min with Reynolds lead citrate.

Samples were examined with a JEOL 100 CX transmission electron microscope. In examining control plants, the vascular tissue in general and the phloem in particular were emphasized. Processes of phloem maturation and the normal structure at different developmental stages were examined. Special efforts were made to identify dense core, filamentoid, and vesicle-like structures similar to those reported for the CPN MLO (11,20,21).

Sampling and processing of plants for manganese comparisons. Samples were taken from symptomless Vero, Bonnie Jean, and Fanfare plants grown without supplemental manganese; from symptomatic tissue of the same cultivars grown with supplemental manganese (1.2, 2.4, and 4.8 g/L $MnSO_4$); from symptomatic tissue of Pink Marble, Florida Marble, and White Marble grown without supplemental manganese; and from symptomatic tissue of Pink Marble and Florida Marble plants grown with supplemental manganese. The position of leaves sampled and all processing were as described above. Samples were compared with respect to cell wall abnormalities, vascular occlusion and collapse, and patterns of necrosis.

RESULTS

Vascular cytology and MLO investigations in control cultivars. Vascular bundles were composed of adaxial xylem with one or two secretory ducts, abaxial phloem, and a surrounding bundle sheath. Xylem parenchyma cells contained an electron-dense particulate substance and vesicles of cytoplasmic origin within central vacuoles. The appearance of the phloem varied widely, depending on the age of the leaf and the size of the vascular bundle. Differences between cultivars were not observed.

Immature phloem in new growth contained differentiating sieve elements filled with cytoplasm, nuclei, ER, dictyosomes, plastids,

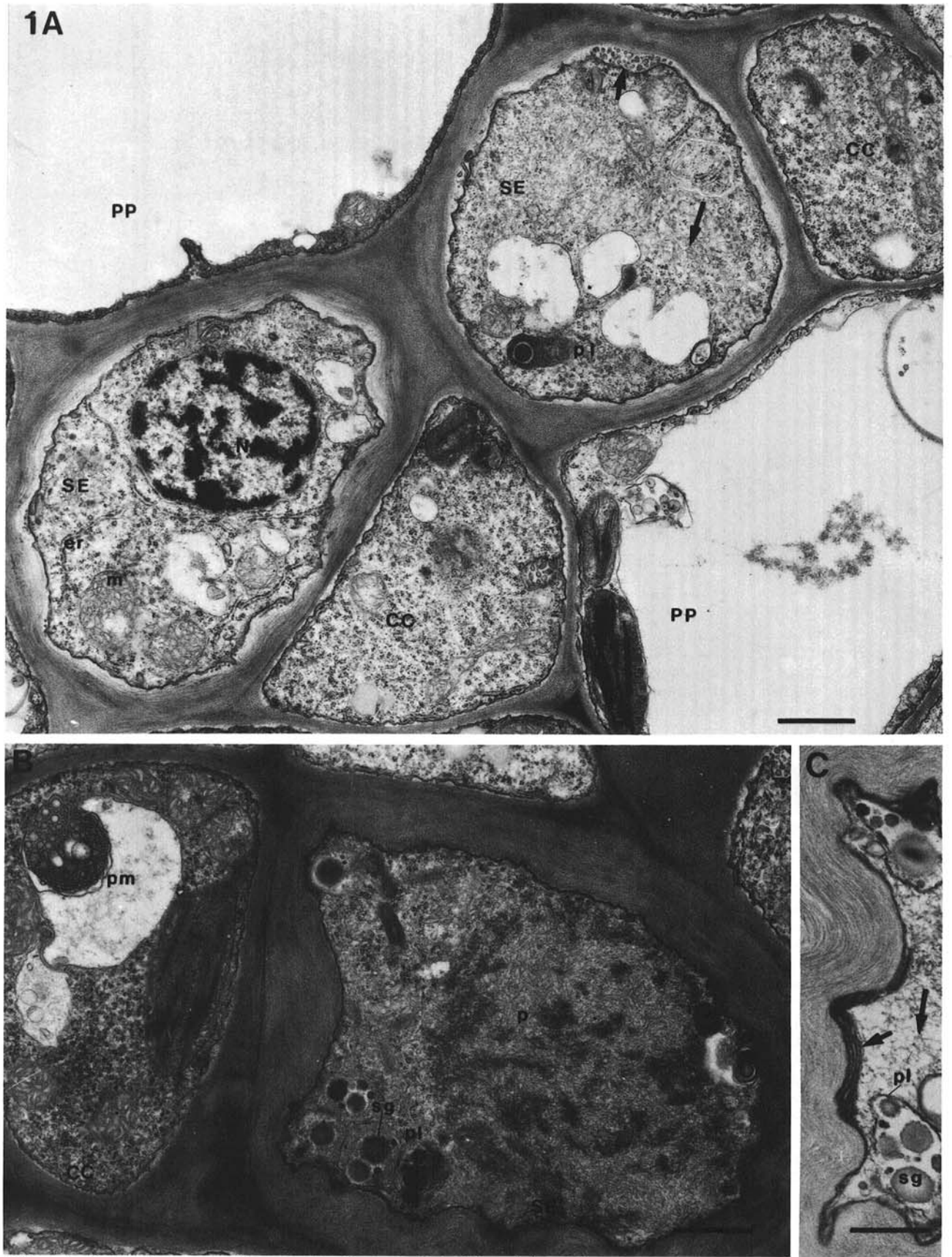

Fig. 1. Phloem in *Dendranthema grandiflora* control cultivars. **A**, Early differentiation of sieve elements, companion cells, and phloem parenchyma in major vein of Vero. Sieve elements contain nuclei, mitochondria, ER, plastids, and numerous vesicles (long arrow). Thickened cell walls contain tubules and vesicles (short arrow) between the plasmalemma and cell wall. **B**, Major vein in Vero with differentiation slightly more advanced than in A. Sieve element contains dispersing P-protein and plastids with electron-dense starch grains. Companion cell contains a paramural body with membranes appearing as either vesicles or tubules, depending on the plane of section. **C**, Mature sieve element in Surf in which tonoplast and many organelles have degenerated. Remaining are fibrous P-protein (long arrow), plastids with starch grains, and parietal filamentoid structures (short arrow), possibly stacks of ER or invaginated plasmalemma. SE, sieve elements; CC, companion cells; PP, phloem parenchyma; N, nuclei; m, mitochondria; er, ER; pl, plastids; pm, paramural body; p, p-protein. Bars = 1, 1, and 0.77 μm for A, B, and C, respectively.

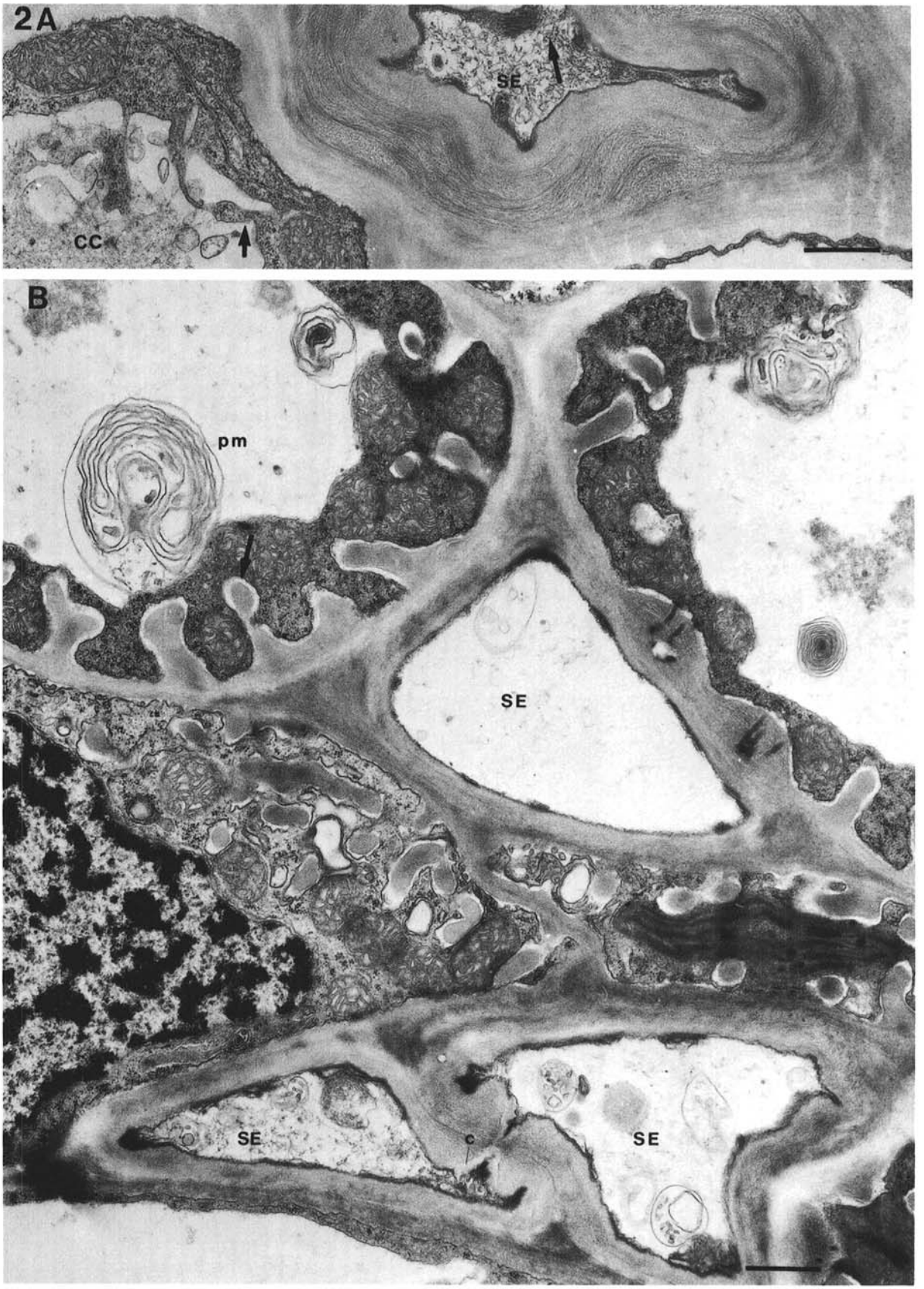

Fig. 2. Mature phloem in *Dendranthema grandiflora* control cultivars. **A**, Major vein in Fanfare. Sieve element has extremely thick cell walls and a small distorted lumen filled with P-protein (long arrow). Cytoplasm in companion cell is vesiculating (short arrow) into central vacuole. **B**, Mature minor vein in Vero. Callose on sieve plates indicate that sieve elements in lower center are no longer functional. Lumens contain remnants of P-protein and degenerating organelles. Cell wall ingrowths (long arrow) are present in parenchyma cells that are not clearly distinguishable as companion or phloem parenchyma cells. Paramural bodies are swollen with separating internal membranes. SE, sieve elements; c, callose; pm, paramural body; CC, companion cell. Bars = 0.76 μm.

mitochondria, P-protein bodies, ribosomes, and vesicles (Fig. 1A and B). Plastids contained osmiophilic granules and electron-dense, round starch grains with smooth or slightly diffuse outlines. In mature sieve elements, nuclei and tonoplasts degenerated, leaving P-protein and starch-filled plastids (Fig. 1C) as well as vesicles, ER, and mitochondria within lumens. Cell walls were often very thick, especially in major veins (Fig. 2A), and callose accumulated on sieve plates (Fig. 2B). Older sieve elements had thinner walls and less content than younger ones. Many appeared empty or contained a few sparse strands of P-protein and remains of degenerating mitochondria, plastids, starch grains, or vesicles (Fig. 2B). In larger bundles with protophloem, sieve elements and companion cells were crushed between phloem parenchyma cells and became permeated with an electron-dense substance.

Phloem parenchyma and companion cells in minor veins had extensive ramiform cell wall ingrowths indicative of transfer cell function (Fig. 2B). Cell wall ingrowths were reduced in number and size in larger veins. Both companion cells and phloem parenchyma contained numerous paramural bodies (Figs. 1B and 2B), which often appeared associated with cell wall ingrowths. In addition to paramural bodies, central vacuoles often contained membrane-bounded vesicles, which appeared to be released through the tonoplast (Fig. 2A).

Vascular cytology in asymptomatic Marble tissue. Vascular tissue was similar to that of control cultivars; however, there were increased accumulations of electron-dense substances in most cell types. Bundle sheath cells contained electron-dense globose substances (Fig. 3A), as well as beaded, filamentoid, or angular

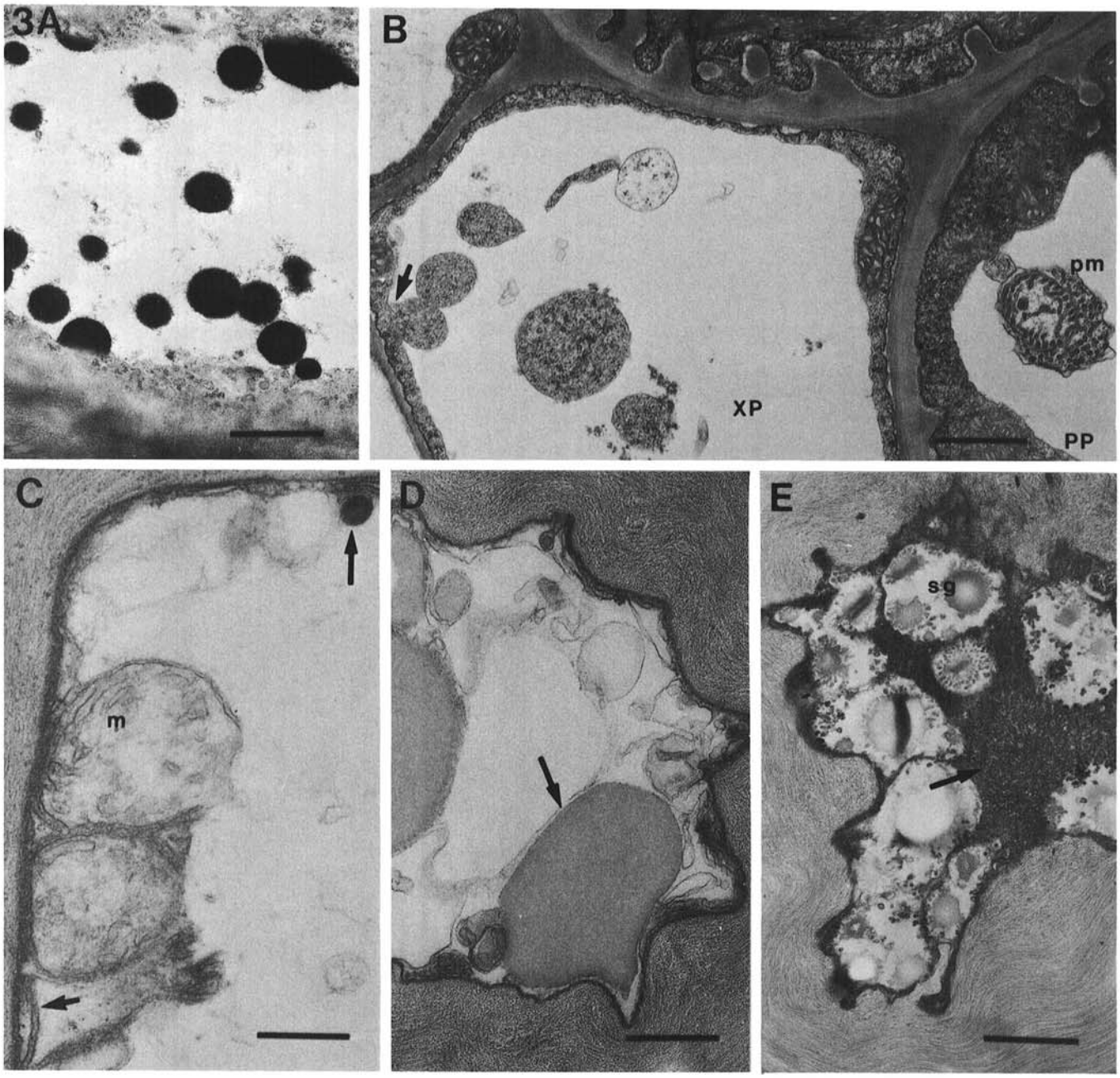

Fig. 3. Vesicular, electron-dense, and filamentoid structures in vascular tissue of *Dendranthema grandiflora* Marble cultivars. **A–C**, symptomless, **D** and **E**, symptomatic. **A**, White Marble bundle sheath cell containing spherical electron-dense globose material in central vacuole. **B**, Florida Marble with vesiculating cytoplasm (short arrow) in xylem parenchyma and paramural body in phloem parenchyma cell. **C**, Sieve element of Florida Marble containing degenerating mitochondria, electron-dense spherical object (small arrow) possibly from plastids (see Fig. 1B), and filamentoid structure (small arrow), possibly ER or remnant of mitochondrian. **D**, Sieve element located close to obliteration in Pink Marble. Electron-opaque structures (arrow) were not observed in controls. **E**, Sieve element from Pink Marble containing plastids and starch grains and an electron-dense matrix not observed in controls. XP, xylem parenchyma; PP, phloem parenchyma; pm, paramural body; sg, starch grains; m, mitochondria. Bars = 1, 1, 0.3, 0.39, and 0.95 μm, respectively.

substances that occasionally pulled out of section. As in healthy controls, xylem (Fig. 3B) and phloem parenchyma cells contained vesicles of host origin in central vacuoles. Numerous paramural bodies occurred in phloem parenchyma (Fig. 3B) and companion cells. Vesicular, filamentoid, and dense core structures in sieve elements appeared to be host components (Fig. 3C) and MLOs were not observed.

Vascular cytology in symptomatic Marble tissue. Extensive accumulations of electron-dense substances similar to those observed in asymptomatic tissues occurred in all cell types. Xylem vessels were sometimes occluded with electron-dense substances, and electron-dense accumulations normally present in xylem parenchyma cells were highly concentrated. Bundle sheath cells were distorted and filled with electron-dense content in central vacuoles, but cytoplasm usually remained intact. Bundle sheath cell walls adjacent to necrotic mesophyll developed membraneous appositions.

Although most vascular cells did not appear necrotic, obliteration of sieve elements and companion cells often appeared enhanced over controls. Intact sieve elements located near obliteration frequently contained electron-opaque structures that were not observed in controls (Fig. 3D). Sieve elements often contained a highly electron-dense matrix in addition to the usual plastids and starch grains (Fig. 3E).

Manganese toxicity investigations. Symptomatic Marble plants grown without supplemental manganese. Necrosis occurred primarily in spongy mesophyll, palisade, and epidermal cells, extending to, but not including, the bundle sheath. Vascular

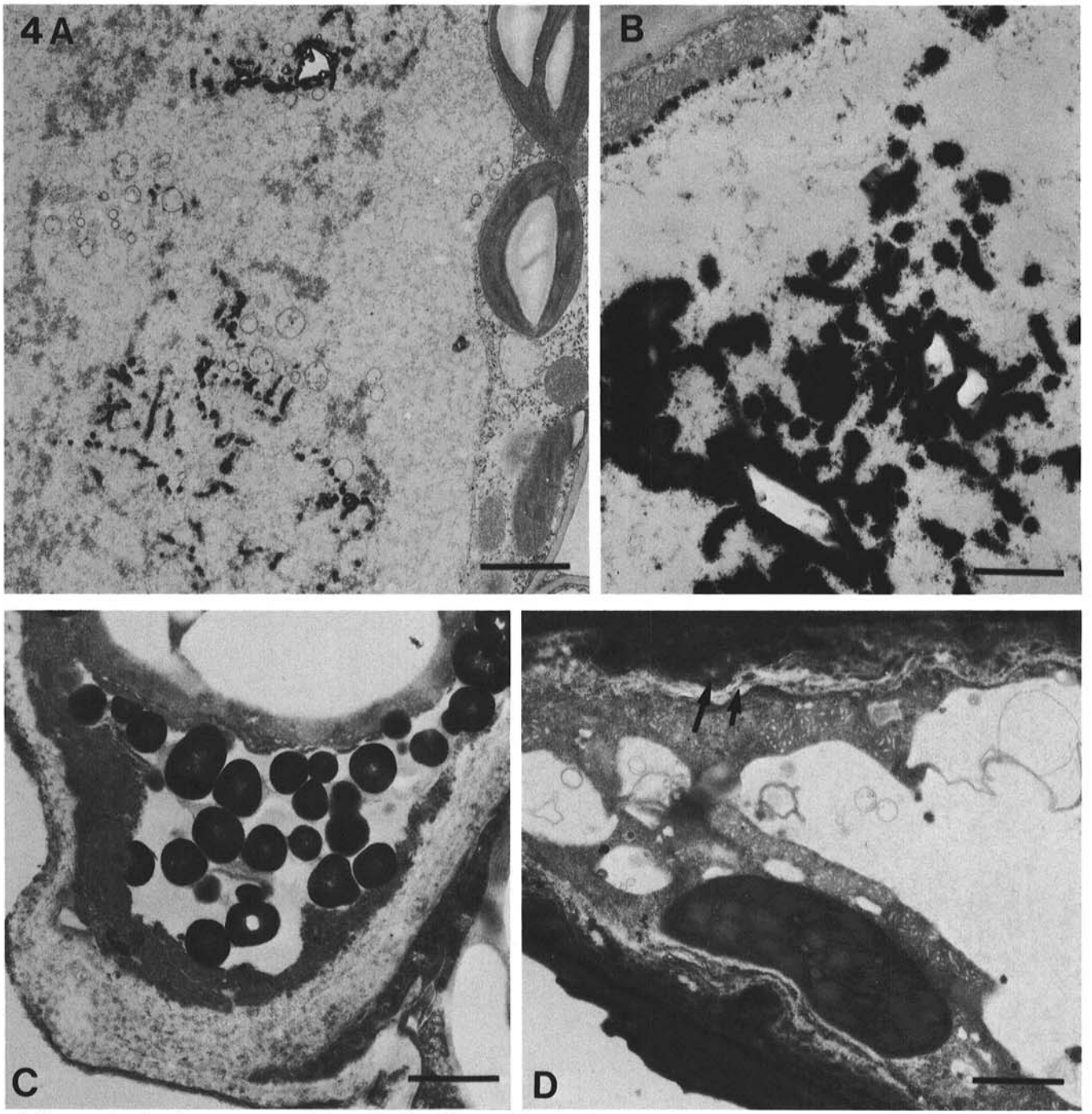

Fig. 4. Nonvascular tissue in or near necrosis in the Marble cultivars of *Dendranthema grandiflora*. **A**, Pink Marble. Palisade cell containing electron-dense beaded filaments aggregated with vesicles and particulate material. **B**, Florida Marble. Epidermal cell with thick electron-dense accumulations in central vacuole. **C**, Florida Marble. Necrotic cell with electron-dense globose accumulations. **D**, Florida Marble. Cell wall apposition in palisade cell bordering necrosis. Appositions often contained electron-dense material adjacent to the wall (long arrow) with that portion distal to the wall more electron-lucent (short arrow). Bars = 1.9, 1, 0.79, and 1.6 μm, respectively.

cytopathology was as described above. Necrotic cells typically had collapsed cell walls, highly electron-dense cytoplasm, and numerous electron-dense substances in vacuoles (Fig. 4A–C). Organelles, especially chloroplasts, occasionally remained recognizable but electron dense.

Walls of cells abutting necrotic cells frequently contained papillae-like wall appositions between the plasmalemma and cell wall (Fig. 4D). Because the bundle sheath was often at the edge of necrosis, appositions commonly developed on bundle sheath cell walls adjacent to collapsed mesophyll. Appositions often formed over plasmodesmata and occurred in the paramural space both as localized semispherical structures extending into the cytoplasm and as more elongate structures circumscribing the wall (Fig. 4D). They contained membranes, fibers, and a moderately stained substance that resembled callose observed on sieve plates. Many appositions were permeated by variable amounts of an electron-dense substance that developed next to the cell wall. In some, pockets of cytoplasm appeared embedded within the apposition. The membrane system occasionally formed regular striations in the apposition, although it more typically appeared convoluted and distorted. Membranes were dilated and contained electron-dense substances.

Manganese toxicity in Vero, Bonnie Jean, and Fanfare. Cytopathological changes associated with manganese were similar to

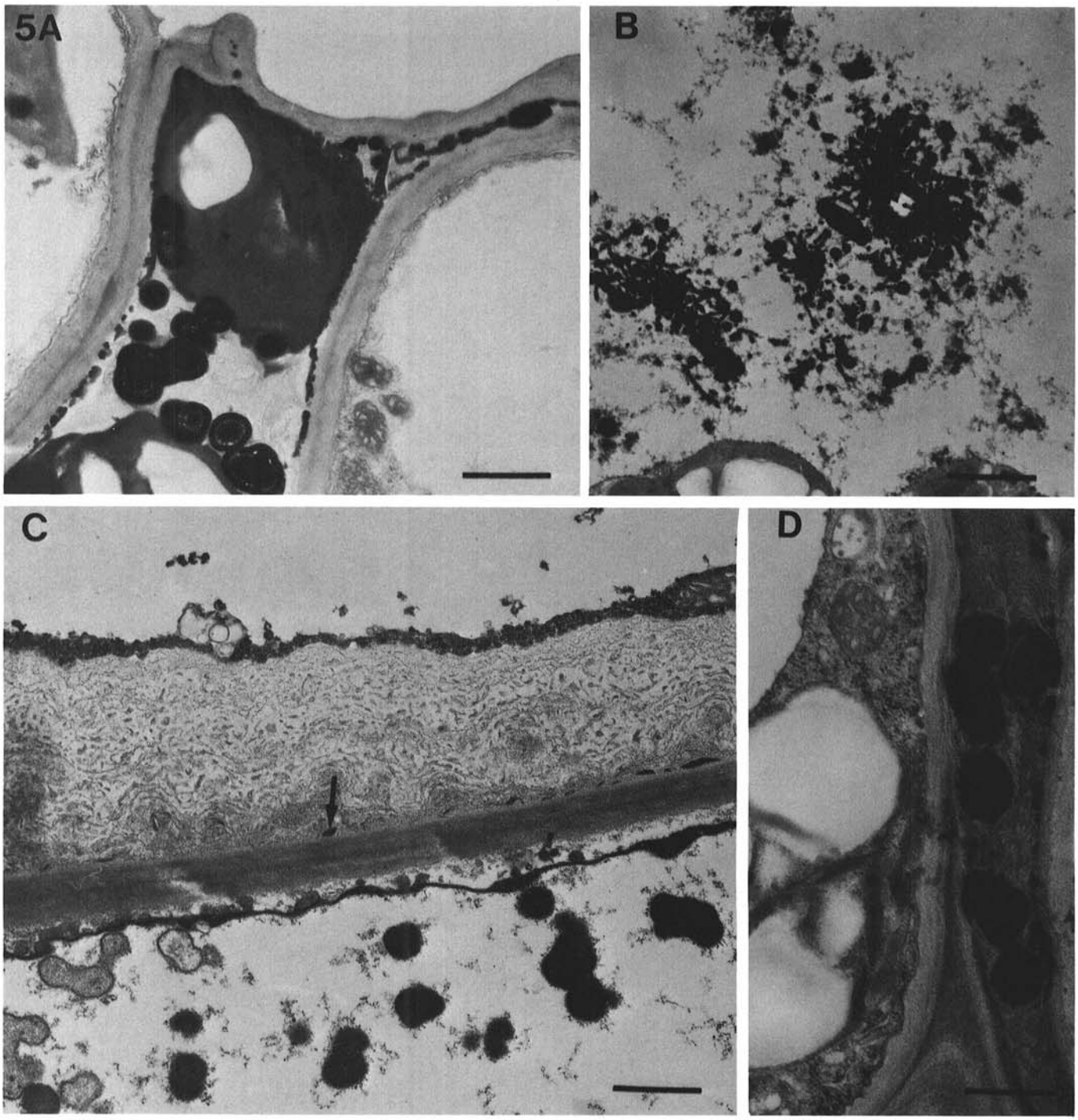

Fig. 5. Cytopathology in manganese-treated control cultivars of *Dendranthema grandiflora* that resembles that in Marble cultivars grown without manganese treatments. **A**, Collapsed spongy mesophyll cell in Vero containing electron-dense globules in central vacuole. **B**, Palisade cell in Vero with electron-dense accumulations in central vacuole. **C**, Bonnie Jean. Cell wall apposition in spongy mesophyll cell showing membranes, fibers, faintly-stained amorphous substance(s), and accumulations of electron-dense substance(s) (arrow) next to wall. **D**, Vero. Electron-dense globular substances in obliterated phloem. Bars = 1.2, 3, 1, and 0.6 μm, respectively.

those observed in untreated, symptomatic tissue from Florida Marble, Pink Marble, and White Marble plants. Cellular collapse and necrosis developed in epidermal, palisade, and spongy mesophyll cells and were often delimited by the bundle sheath. Necrotic cells displayed electron dense cytoplasm, distorted cell walls, and electron-dense globules in central vacuoles (Fig. 5A). Vacuoles of intact cells were filled with beaded, globular, tubular, and angular electron-dense substances (Fig. 5B). These structures were indistinguishable from those present in the Marble cultivar. Xylem vessels were filled with electron dense particulate. Appositions developed on walls of cells abutting necrotic cells (Fig. 5C).

The extent of vascular degeneration was variable, appearing extensive in some cases and minimal in others. In Vero, an electron-dense globose substance was observed in collapsed sieve elements and companion cells within protophloem (Fig. 5D). Obliterating sieve elements developed opaque structures similar to those previously seen only in the Marble cultivars.

Effects of high manganese levels on vascular tissue of all cultivars. High manganese levels (4.6 g/L $MnSo_4$) produced a type of vascular degeneration that was not observed at lower levels. An electron-dense particulate filled the phloem, appearing between plasmalemmae and cell walls and within central vacuoles. Paramural bodies over companion cell wall ingrowths filled with particulate and the network of wall ingrowths appeared less extensive and ramiform (Fig. 6A). In some cases, the entire metaphloem collapsed (Fig. 6B).

DISCUSSION

Plants of the Marble cultivars used in this study displayed cytopathological features similar to those previously described by Israel et al (11) and McGovern et al (20–22) for CPN-infected plants, with two exceptions. MLOs were not observed and phloem necrosis was not a consistent feature. Other features, such as mesophyll collapse, occlusion of xylem vessels, increased production of possible tannins, and formation of cell wall appositions, were apparently indistinguishable. Given the same cultivars, symptoms, and cytopathology, it appears likely that, at least to some extent, we are describing the same syndrome. Plants known to be positive for CPN were not available during the course of this study for the side-by-side comparison that would resolve the question.

Comparing the two syndromes, using published descriptions and micrographs of the CPN agent alone, was complicated by the lack of information on healthy controls in these reports (11,20–22). The CPN MLO reportedly appears in three forms: vesicular, dense-core, and filamentoid (11,20). However, many of the vesicular, filamentous, and electron-dense spherical structures that we observed in our controls were not included in descriptions of healthy controls in CPN studies. For example, control sieve elements were reported to contain only P-protein (21) but, in our controls, we also observed spherical electron-dense bodies (starch grains), vesicles (degenerating plastids and mitochondria), and filamentoid structures (ER and plasmalemmae). These organelles were discernable in developing sieve elements, and their continued presence in mature sieve elements has been previously documented (5–7,26).

Although we did not observe structures in sieve elements that resembled the vesicular and electron-dense CPN MLO profiles, we did see similar structures in phloem and xylem parenchyma cells, where the MLO also is reported to occur (11,21). However, because these also occurred in control cultivars, they appeared to be host components. In phloem, filamentous structures appeared to be remnants of lysed paramural bodies. Vesicles, in numerous cell types, including xylem and phloem, originated from host cytoplasm. Most of the latter contained cytoplasmic remnants and appeared to be autophagic vesicles (5,19), a feature that may be prominent in the phloem parenchyma (5). Still other vesicles, with little apparent content, appeared similar to vesicles involved in solute transport (29).

Dense-core MLOs (11) also appeared similar to structures we interpreted as host components. Initially we only saw these components in the Marble cultivars, although not in sieve elements. They were subsequently observed in control cultivars stressed by excess levels of manganese. Although identifying them chemically was beyond the scope of this study, electron-dense host vacuolar components similar to the substances we observed have been previously described as tannins (5,19) and vacuolar proteins (19). Tannins, which are present in elevated concentrations in the Marble cultivars (11,20), may appear in vacuoles as particles in various states of aggregation and as large spherical structures without membranes (5,19). Proteinacious deposits also may form electron-dense spheres (19). In addition to tannins and proteins, the angular shape of some electron-dense forms suggests a crystalline composition, whereas the affinity for osmium may indicate a lipid or suberin constituent. In some necrotic cells, spherical structures may represent degenerating cytoplasm, phenolic substances, or other degradative products. Many of these bodies (or substances) might be misinterpreted as MLOs, especially when visible as beaded filaments. Although we have interpreted them and other dense-core, vesicular, and filamentous structures as host components, the resemblance of all these structures to MLOs

Fig. 6. Effects of high (4.6 g/L) levels of manganese on vascular tissue of *Dendranthema grandiflora* cultivars. **A**, Florida Marble. Companion cell damage reflected by electron-dense particulate permeating central vacuole, paramural spaces (short arrow), and paramural bodies (long arrow) over cell wall ingrowths. **B**, Metaphloem collapse in Fanfare. SE, sieve elements; CC, companion cell; PP, phloem parenchyma cell. Bars = 0.76 and 1.6 μm for A and B, respectively.

underscores the need for caution when relying on EM results to confirm (or rule out) the presence of an MLO.

Unlike CPN-affected Marble cultivars (20–22), phloem necrosis and premature sieve element obliteration were not consistent features in the Marble cultivars in this study, although they did occur. Other reported vascular effects, including occlusion of xylem vessels (20,21), also were present. We did not interpret this as diagnostic of CPN, however, because we observed collapsed phloem and occluded xylem vessels in all cultivars when high levels of manganese were applied. The damage to the phloem we observed may reflect the important role phloem plays in recycling solutes to prevent their toxic buildup. In minor veins, phloem transfer cells specifically are thought to minimize damage by retrieving solutes from the xylem and subsequently loading the sieve elements for export out of the leaf (24,30). Although cell wall ingrowths on transfer cells (23) and plasmatubules in paramural spaces (9) enable these cells to efficiently move solutes from apoplast to symplast, excessive salt levels will eventually damage transfer cells and interfere with recycling (30). This may explain our observations that transfer companion cells sometimes appeared more abnormal than sieve elements.

The formation of papillae-like cell wall appositions represents another characteristic common both to manganese-stressed chrysanthemums and to those infected with the putative CPN MLO. Again, we did not interpret this as necessarily indicative of a pathogen since these appositions apparently function to sequester damaged or wounded tissue, regardless of the presence or absence of a pathogen (1,27). Such appositions may display considerable variability in appearance and structure, but many reports describe similar forms to those we observed (1,2,10,32). Content ascribed to these appositions include phenolic substances, fibers, membranes, entrapped cytoplasm, and callose. Our preliminary tests with the nitroso reaction have indicated that electron-dense areas adjacent to the walls are rich in phenolic material (4). Other work, with aniline blue, indicated that the portions of appositions distal to the wall contain callose (17). Although aniline blue is not specific for callose, it does have a high affinity for it (27), and our ultrastructural observations support this identification. Aniline blue-positive material in appositions appeared as a faintly stained amorphous substance similar to callose described in other cell wall appositions (2,28) and indistinguishable to that we observed on sieve plates and plasmodesmata.

Although wall appositions may be a generalized host defense, in this case there may also be a direct link with manganese toxicity. Excess manganese has been previously implicated in the formation of callose and, in manganese-sensitive cowpea, callose accumulations may even be an earlier indication of toxicity than necrosis (31). Callose formation, which requires calcium (1,3,14,15), follows plasmalemma disturbances (3,12,14,15), and is thought to occur when an influx of calcium into the cell through damaged membranes activates B 1-3 glucan synthase on the plasmalemmae (3,12,14,15). Manganese is apparently able to substitute for calcium in many plant species (8), and divalent cations, including manganese and magnesium, can activate at least one B 1-3 glucan synthase directly (23). Because manganese is transported primarily in the apoplast (8), the speculation that excess levels can damage the plasmalemma and trigger callose production (31) is supported by our observations of numerous cell wall abnormalities in chrysanthemums affected by manganese toxicity.

In conclusion, many responses previously attributed to an MLO in the Marble cultivars may instead represent a stress reaction. This reaction is indistinguishable from that in other cultivars with confirmed cases of manganese toxicity, providing supporting evidence for data indicating that the Marble cultivars are highly sensitive to manganese (17). However, previous reports of MLOs in the Marble cultivars were based on an exhaustive investigation that used many different approaches to support ultrastructural identification of an MLO (20). Until side-by-side comparisons are undertaken with definite CPN positives, the possibility that CPN represents a distinct syndrome with an etiology different from CFN cannot be ruled out.

LITERATURE CITED

1. Aist, J. R. 1983. Structural responses as resistance mechanisms. Pages 33-70 in: The Dynamics of Host Defense. J. A. Bailey and B. J. Deverall, eds. Academic Press, New York. 233 pp.
2. Brammall, R. A., and Higgins, V. J. 1987. The effect of glyphosphate on resistance of tomato to fusarium crown and root rot disease and on the formation of host structural defensive barriers. Can. J. Bot. 66:1547-1555.
3. Delmar, D. P., Thelen, M., and Marsden, M. P. F. 1984. Regulatory mechanisms for the synthesis of B-glucans in plants. Pages 133-149 in: Structure, Function and Biosynthesis of Plant Cell Walls. W. M. Dugger and S. Bartnicki-Garcia, eds. Proc. Ann. Symp. Bot. 7th.
4. Dienelt, M. M., and Lawson, R. H. 1989. Manganese toxicity in the Marble cultivars of *Chrysanthemum morifolium*. II. Electron microscopy. (Abstr.) Phytopathology 79:1149.
5. Esau, K. 1978. Developmental features of the primary phloem in *Phaseolus vulgaris* L. Ann. Bot. 42:1-13.
6. Esau, K., and Cheadle, V. I. 1965. Cytologic studies on phloem. Univ. Calif. Publ. Bot. 36:253-343.
7. Evert, R. F. 1984. Comparative structure of phloem. Pages 145-234 in: Contemporary Problems in Plant Anatomy. R. A. White and W. C. Dickison, eds. Academic Press, New York. 598 pp.
8. Foy, C. D. 1983. The physiology of plant adaption to mineral stress. Iowa State J. Res. 57:355-391.
9. Harris, N., and Chaffey, N. J. 1985. Plasmatubules in transfer cells of pea (*Pisum lativum* L.). Planta 165:191-196.
10. Heitefuss, R., and Ebrahim-Nesbat, F. 1986. Ultrastructural and histochemical studies on mildew of barley (*Erysiphe graminis* DC. f. sp. *hordei* Marchal) III. Ultrastructure of different types of papillae in susceptible and adult plant resistant leaves. J. Phytopathol. 116:358-373.
11. Israel, H. W., Horst, R. K., McGovern, R. J., Kawamoto, S. O., Weaber, K. F., Bucci, S. J., and Paduch-Cichal, E. 1988. Chrysanthemum phloem necrosis: Microscopy of the putative pathogen. Acta Hortic. 234:145-155.
12. Jacob, S. R., and Northcote, D. H. 1985. In vitro glucan synthesis by membranes of celery petioles: The role of the membrane in determining the type of linkage formed. J. Cell Sci. Suppl. 2:1-11.
13. Kahn, R. P., Lawson, R. H., Monroe, R. L, and Hearon, S. 1972. Sweet potato little-leaf (Witches'-broom) associated with a mycoplasmalike organism. Phytopathology 62:903-909.
14. Kauss, H. 1985. Callose biosynthesis as a Ca^{2+}-regulated process and possible relations to the induction of other metabolic changes. J. Cell Sci. Suppl. 2:89-103.
15. Kohle, H., Wolfgang, J., Frauke, P., Wolfgang, B., and Kauss, H. 1985. Chitosan-elicited callose synthesis in soybean cells as a Ca^{2+}-dependent process. Plant Physiol. 77:544-551.
16. Lawson, R. H., and Dienelt, M. M. 1989. Manganese toxicity in the Marble cultivars of *Chrysanthemum morifolium*. I. Cytochemistry. (Abstr.) Phytopathology 79:1148-1149.
17. Lawson, R. H., and Dienelt, M. M. 1991. Chrysanthemum foliar necrosis: Symptoms, histochemistry, and X-ray analysis of leaf lesions. Phytopathology 81:1071-1078.
18. Lawson, R. H., and Dienelt, M. M. Heat induced abnormalities in the flowers of the Marble cultivars of *Chrysanthemum morifolium*. (Abstr.) Phytopathology 80:978.
19. Matile, P. 1975. The Lytic Compartment in Plant Cells. Springer-Verlag, New York. 183 pp.
20. McGovern, R. J. 1986. Studies on chrysanthemum phloem necrosis. Ph.D. thesis. University Microfilms International #8623168. Cornell University, Ithaca, NY. 135 pp.
21. McGovern, R. J., Horst, R. K., and Israel, H. W. 1989. Chrysanthemum phloem necrosis: Symptomatology and histopathology. Can. J. Bot. 67:1014-1023.
22. McGovern, R. J., Horst, R. K., and Israel, H. W. 1989. Chrysanthemum phloem necrosis: Detection by epifluorescence microscopy. Can. J. Bot. 67:1024-1031.
23. Morrow, D. L., and Lucas, W. J. 1986. (1-3)-B-D-glucan synthase from sugar beet. Plant Physiol. 81:171-176.
24. Pate, J. S., and Gunning, B. E. S. 1969. Vascular transfer cells in angiosperm leaves. A taxonomic and morphological survey. Protoplasma 68:135-156.
25. Post, K., and Lacey, D. B. 1951. High temperature produces long day effect on chrysanthemum. N.Y. State Flower Grow. Bull. 76:4-5,8.
26. Spanner, D. C., and Jones, R. L. 1970. The sieve tube wall and its relation to translocation. Planta 92:64-72.

27. Stone, B. A. 1984. Noncellulosic B-glucans in cell walls. Pages 52-74 in: Structure, Function, and Biosynthesis of Plant Cell Walls. W. H. Dugger and S. Bartnicki-Garcia, eds. Proc. Ann. Symp. Bot. 7th.
28. Tighe, D. M., and Heath, M. C. 1982. Callose induction in cowpea by uridine diphosphate glucose and calcium phosphate-boric acid treatments. Plant Physiol. 69:366-370.
29. Van Steveninck, R. F. M., Van Steveninck, M. E., Peters, P. D., and Hall, T. A. 1976. Ultrastructural localization of ions. IV. Localization of chloride and bromide in Nitella translucens and X-ray energy spectroscopy of silver precipitation products. J. Exp. Bot. 27:1291-1312.
30. Winter, E. 1982. Salt tolerance of trifolium alexandrinum L. III. Effects of salt on ultrastructure of phloem and xylem transfer cells in petioles and leaves. Aust. J. Plant Physiol. 9:239-250.
31. Wissemeier, A. H., and Horst, W. J. 1987. Callose deposition in leaves of cowpea (*Vigna unguiculata* (L.) Walp.) as a sensitive response to high Mn supply. Plant Soil 102:283-286.
32. Zeyen, R. J., and Bushnell, W. R. 1978. Papilla response of barley epidermal cells caused by *Erysiphe graminis*: Rate and method of deposition determined by microcinematography and transmission electron microscopy. Can. J. Bot. 57:898-913.